International Journal of Fluid Power 12 (2011) No. 1 pp. 41-50

EFFECTS OF MANUFACTURING DEVIATION ON THE PRESSURE PULSATION OF THREE SCREW PUMPS

Sunghun Kim, Ulf Piepenstock and Hubertus Murrenhoff

RWTH Aachen University, Institute for Fluid Power Drives and Controls, Steinbachstr. 53, 52074 Aachen, Germany
sung-hun.kim@ifas.rwth-aachen.de, ulf.piepenstock@ifas.rwth-aachen.de, hubertus.murrenhoff@ifas.rwth-aachen.de

Abstract

When both, a low operating pressure and an extremely low pulsation is required screw pumps can be better than other machines. Due to their low pulsation, low noise level, good suction ability and high reliability, screw pumps are often the best solution. It is shown in this paper that pumps can vary in pressure pulsation very much depending on manufacturing deviations. Therefore this paper deals with a simulation model, which was verified by experimental tests. Then the calculated pressure pulsation according to cylindrical, conical and eccentric deviation in dimension of the manufactured parts from the design is presented. Precisely, each difference in pulsation characteristic can be explained with manufacturing deviations. Three screw pumps are very sensitive to eccentricity and pressure pulsation can be reduced by using the optimal length of the drive spindle. Additionally, the positive impact of a conical spindle is shown.

Keywords: screw pump, pulsation, manufacturing deviation, RALA

1 Introduction

Three screw pumps have no kinematic pulsation (Willibald, 1992) and generate low fluid-borne and air-borne noise because the pressure of a chamber increases gradually by leakage while the chamber is moved from the suction port to the discharge port. This is similar to gear or vane pumps. Screw pumps have a good suction ability due to comparable low pressure losses at the suction port of the pump. The reliability is high, provided by a hydrodynamic pressure between the spindles, which causes a balance in the pump (Geimer, 1995). Due to these advantages, three screw pumps are used for noise- and pulsation-sensitive applications, such as casting machines, machine tools and broaching machines.

In this study it proved problematic that, although the pumps are of the same type and from the same manufacturer, the characteristic of pressure pulsation is different as shown by Fig.1. For example, the pressure pulsation of pump C is about three times higher than the pulsation of pump B.

Since the three screw pump was invented by Imo Pump, there have been many experimental researches (Feist, 1976; Willibald, 1992) and theoretical researches with experiments (Wegener, 1985; Geimer, 1995; Ryanzantsev, 2000) but yet no research which could explain this observation.

This manuscript was received on 26 March 2010 and was accepted after revision for publication on 10 February 2011

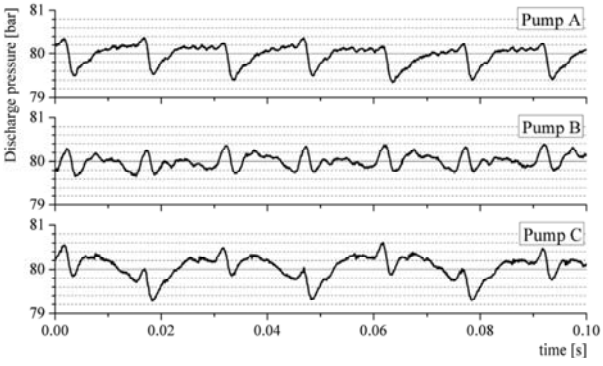

Fig. 1: *Discharge pressure pulsation of three different screw pumps of the same type*

This paper shows that manufacturing deviations can be the reason for this. The effects of manufacturing deviations on the pressure pulsation were studied in order to improve the reliability and the performance of three screw pumps.

The specifications of the pump used in this study are shown by Table 1.

Table 1: Specifications of the three screw pumps used in this study

Volumetric displacement [cc/rev]	50
Rated rotation speed [rpm]	2000
Rated discharge pressure [bar]	80
Pitch [mm]	78

2 Simulation Model

Generally, the pressure change of a chamber in a pump can be epressed as follows:

$$\frac{dp_c}{dt} = \frac{E_{Fl}}{V_c}\left\{Q_c - Q_L - \frac{dV_c}{dt}\right\} \quad (1)$$

In this equation E_{Fl} is the effective bulk modulus of the oil, V_C is the volume of a chamber, Q_C is the flow between a chamber and inlet or outlet port, Q_L is leakage and p_c is the pressure of a chamber.

So, the simulation of the pressure pulsation of a three screw pump requires knowledge about the values in Eq. 1.

2.1 Chamber Volume and Port Connection

In three screw pumps the displacement chamber is formed by a drive spindle, two idle spindles and the sleeve of the pump. So, a chamber in a three screw pump consists of two spaces formed by the drive spindle and the sleeve (C_{ds}) and two spaces formed by the idle spindle and the sleeve (C_{is}) as can be seen in Fig. 2.

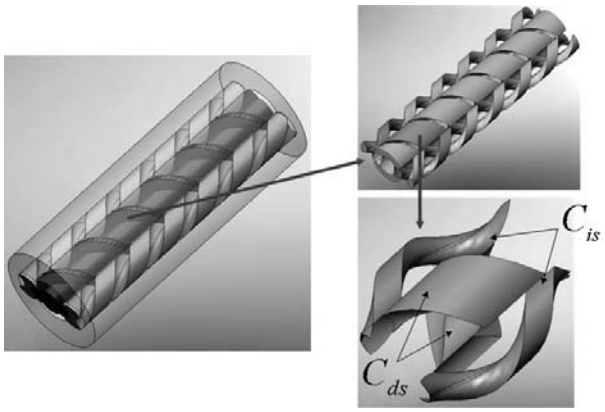

Fig. 2: *Displacement chamber of a three screw pump*

While the drive spindle meshes with both idle spindles, the displacement chambers deliver fluid from the low pressure inlet to the high pressure outlet. Precisely, as illustrated in Fig. 3, the chambers appear at rotation angles of 180°×n (n = 1, 2, 3…). The formation of the first displacement chamber starts at the inlet at a rotation angle of (180°-α), where point 5 of the drive spindle is in contact with point 6 of an idle spindle. The chamber is separated from the inlet at the rotation angle (540°+α) and the closed chamber is moved to the high pressure port. Due to leakage between the displacement chambers the pressure rises gradually. The pressure chamber begins to open to the outlet at a rotation angle of (θ_l - 180°×n) and discharges fluid.

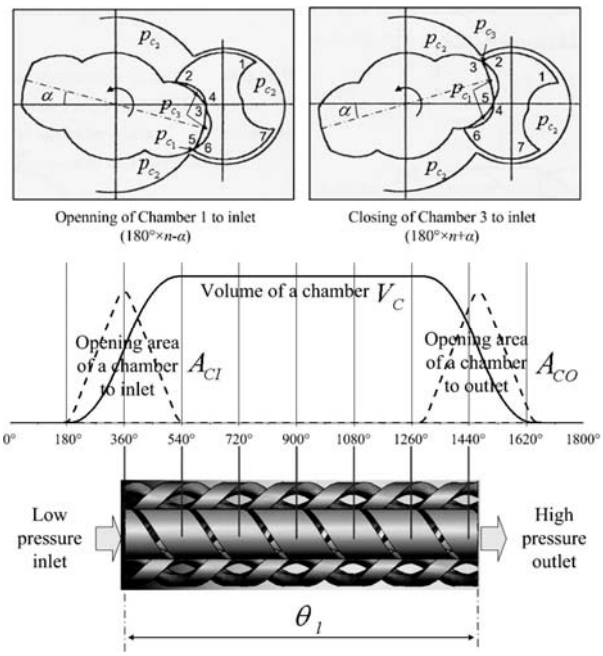

Fig. 3: *Variation of chamber volume and opening areas*

The flow between a chamber and the ports is given by:

$$Q_{Ci} = \alpha_D\left(A_{CI_i}\sqrt{\frac{2(p_s - p_{c_i})}{\rho}} + A_{CO_i}\sqrt{\frac{2(p_d - p_{c_i})}{\rho}}\right) \quad (2)$$

In this formula p_s is the suction pressure and p_d is the discharge pressure.

2.2 Leakage

The leakage in three screw pumps can be divided into 4 parts according to the following definitions (Geimer, 1995):

- Leakage between $C_{ds(n)}$, $C_{ds(n+1)}$ and $C_{ds(n-1)}$ through the gap between the sleeve and the outside of the drive spindle - laminar flow (*L1*);
- Leakage between $C_{is(n)}$, $C_{is(n+1)}$ and $C_{is(n-1)}$ through the gap between the sleeve and the outside of the idle spindles - laminar flow (*L2*);
- Leakage between $C_{ds(n)}$, $C_{ds(n+1)}$ and $C_{ds(n-1)}$ through the gap between the inside of a drive spindle and outside of the idle spindles - turbulent flow (*L3*);
- Leakage between $C_{is(n)}$, $C_{is(n+2)}$ and $C_{is(n-2)}$ through the gap between the outside of the drive spindle and inside of the idle spindles - turbulent flow (*L4*).

As can be seen in Fig. 4, chamber *n* is connected with chamber *n* + 1 and chamber *n*-1 by *L1*, *L2* and *L3*. It is also connected with a chamber *n* + 2 and a chamber *n* - 2 by *L4*.

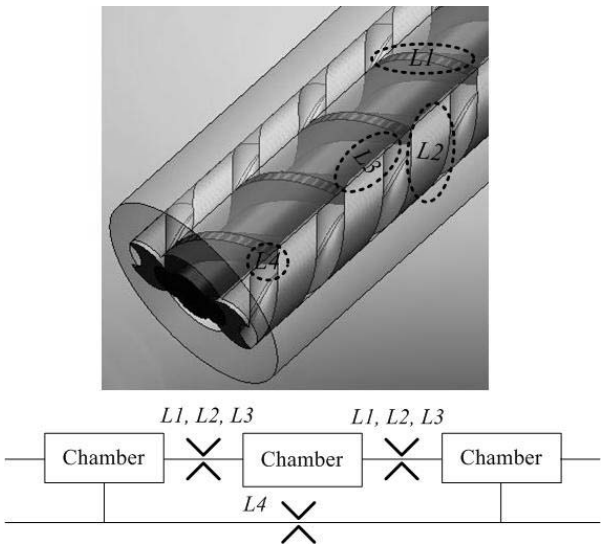

Fig. 4: *Leakage in a three screw pump*

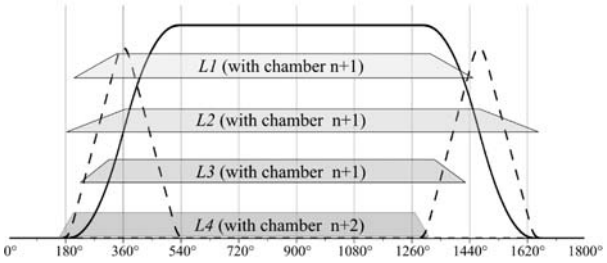

Fig. 5: *Gap width changes of L1, L2, L3 and L4*

Each gap width variation of *L1*, *L2, L3* and *L4* must be considered in the simulation model because the positions of formation and deformation of gaps are different which are formed by the drive spindle, two idle spindles and the housing. For example, *L1* starts at the rotation angle when the outside of the drive spindle of chamber *n* gets into contact with the sleeve. *L2* starts when the idle spindle has rotated 180°× n, *L3* begins at the rotation angle when $C_{ds(n)}$ has begun to grow and *L4* starts at the rotation angle when $C_{is(n)}$ is formed. Fig. 5 shows the gap width variations of *L1*, *L2, L3* and *L4*.

The leakages *L1*, *L2, L3* and *L4* can be expressed as follows:

$$Q_{\mathrm{L1_i}} = \frac{l_{1_{i-1}} h_{1_{i-1}}^{\ 3}}{12\eta b}(p_{c_i} - p_{c_{i-1}}) + \frac{l_{1_i} h_{1_i}^{\ 3}}{12\eta b}(p_{c_i} - p_{c_{i+1}}) \qquad (3)$$

$$Q_{\mathrm{L2_i}} = \frac{l_{2_{i-1}} h_{2_{i-1}}^{\ 3}}{12\eta b}(p_{c_i} - p_{c_{i-1}}) + \frac{l_{2_i} h_{2_i}^{\ 3}}{12\eta b}(p_{c_i} - p_{c_{i+1}}) \qquad (4)$$

$$Q_{\mathrm{L3_i}} = \alpha_{\mathrm{D}} \left(h_{3_{i-1}} \cdot l_{3_{i-1}} \sqrt{\frac{2(p_{c_i} - p_{c_{i-1}})}{\rho}} + h_{3_i} \cdot l_{3_i} \sqrt{\frac{2(p_{c_i} - p_{c_{i+1}})}{\rho}} \right) \qquad (5)$$

$$Q_{\mathrm{L4_i}} = \alpha_{\mathrm{D}} \left(h_{4_{i-2}} \cdot l_{4_{i-2}} \sqrt{\frac{2(p_{c_i} - p_{c_{i-2}})}{\rho}} + h_{4_i} \cdot l_{4_i} \sqrt{\frac{2(p_{c_i} - p_{c_{i+2}})}{\rho}} \right) \qquad (6)$$

In those equations l is the gap width, h is the gap height, η is the dynamic viscosity, ρ is the density, b is the thickness of the idle spindle and α_{D} is the orifice coefficient.

2.3 Simulation Model

As was stated above, the simulation model for the pump used in this paper consists of 10 chambers due to the length of the drive spindle as Fig. 3 shows. The chambers are connected by leakage paths and divided at a separation point.

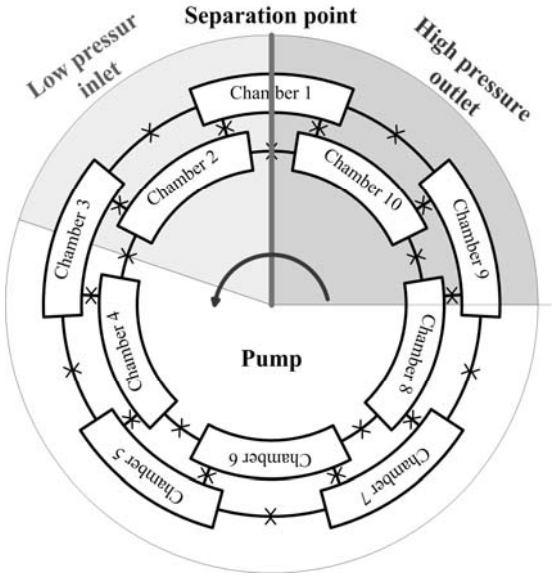

Fig. 6: *Schematic diagram of the simulation model*

Figure 6 illustrates the simulation model, the current situation shows:

- chamber 3 is connected to the inlet
- chambers 4, 5, 6 and 7 are closed
- chambers 9 and 8 are connected to the outlet
- imaginary volumeloss chambers 1, 2 and 10

3 Verification of the Simulation Model

3.1 Experimental System

To measure the pressure pulsation of the three screw pumps, an existing test stand was used. It consists of the test pump, pressure sensors, a temperature sensor, reflectionless line termination (RALA), a filter, a pressure relief valve, a flow sensor, and a circulation unit as shown by Fig. 7.

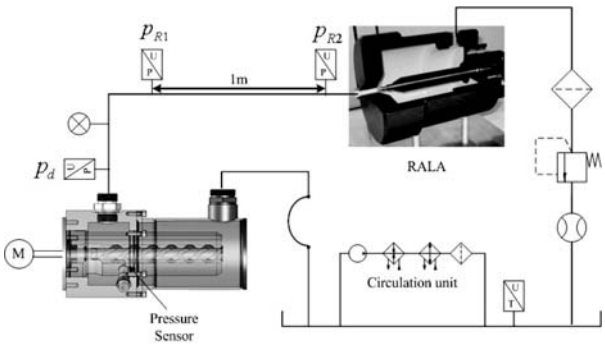

Fig. 7: *Arrangement of test stand*

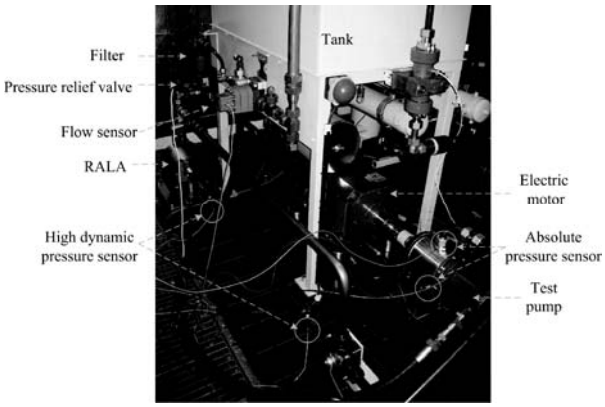

Fig. 8: *Experimental system*

The test rig is equipped with a measuring section for flow ripples and pressure pulsations. Therefore, a RALA is installed. It is necessary to avoid reflections of the pressure ripples. To adjust the RALA, high-dynamic pressure sensors to measure p_{R1} and p_{R2} are needed. Fig. 9 shows a good setup and operation of the RALA.

In order to verify the computed results, not only the outlet pressure pulsation was measured using an absolute pressure sensor in the pipe, but also the pressure inside of the displacement chamber before being connected to the outlet. For this purpose an absolute pressure sensor was integrated into the pump.

The test pump is driven by an electric motor and the discharge pressure is controlled by the RALA and the pressure relief valve.

The temperature of the experimental system was kept constant at 40 °C by the circulation unit.

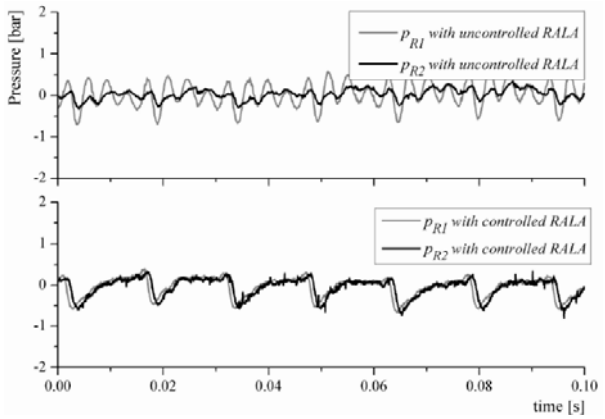

Fig. 9: *Pressure pulsation of* p_{R1} *and* p_{R2}

3.2 Simulation Program

As illustrated in Fig. 10, the simulation model of a three screw pump was realized using DSH*plus*, a simulation program to model hydraulic systems.

The following parameters were entered into the simulation program using look-up tables and dependent on the rotation angle:

- Volume of chambers;
- Opening area of chambers to inlet and outlet;
- Gap width of *L1*, *L2*, *L3* and *L4*.

The RALA was modelled as an orifice.

So, the discharge pressure of a three screw pump can be calculated with Eq. (7).

$$\frac{dp_d}{dt} = \frac{E_{Fl}}{V_d}\alpha_D \left\{ \sum A_{CO_i} \sqrt{\frac{2\cdot(p_O - p_{c_i})}{\rho}} - \sqrt{\frac{2(p_d - p_2)}{\rho}} \right\} \quad (7)$$

Here p_2 is the pressure between the RALA and the pressure relief valve.

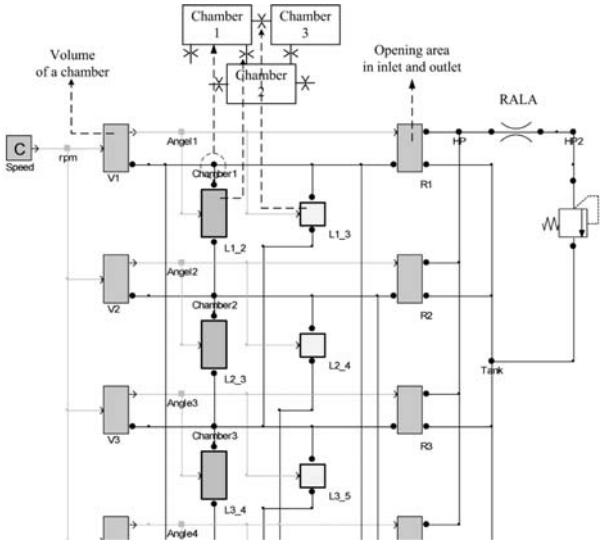

Fig. 10: *DSHplus simulation model*

3.3 Results

In this study, experiments and simulations were carried out at a rotation speed of 2000 rpm and a discharge pressure of 80 bar. The values are rated rotation speed and load pressure of the test pump.

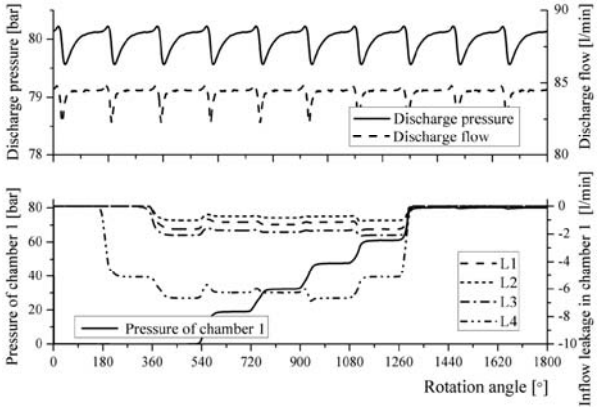

Fig. 11: *Computed results*

Figure 11 shows the computed results which are discharge flow and pressure, pressure inside a chamber from inlet to outlet and leakage. In this calculation the gap heights were assumed as 65 μm for *L1* and *L2*, 20 μm for *L3* and 70 μm for *L4*. The values were chosen with the help of the measurement of discharge pressure and the pressure of the last chamber.

As shown by Fig. 11, a three screw pump has two pressure pulsations per revolution because the chambers appear at the rotation angles (180°× *n*). The pressure in the closed displacement chamber rises stepwise due to the leakage. With these computed results it is understandable, that there is a relatively large undershoot of the discharge pressure when the chamber is opened to the outlet and a small overshoot before. This behavior will be explained in detail in the following chapter.

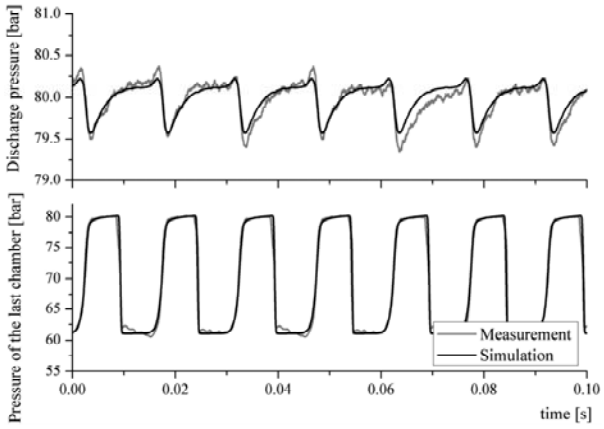

Fig. 12: *Comparison of computed results with experimental results*

The calculated discharge pressure and the pressure of the last chamber are compared with experimental results in Fig. 12. This figure demonstrates that in this study the computed results of the simulation model match very well with measurements.

4 Causes of Pulsation

For a better understanding about the pressure pulsation of a three screw pump, causes of pulsation in the pump must be analyzed. In this chapter, causes of a discharge flow pulsation are analyzed because a flow pulsation causes pressure pulsation.

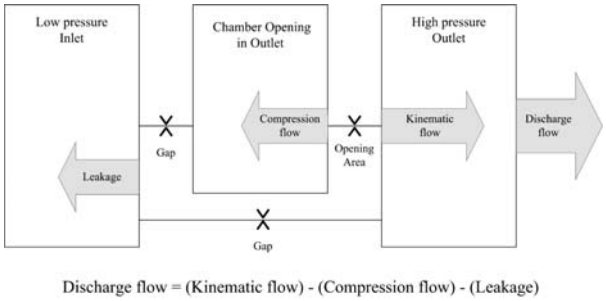

Fig. 13: *Diagram of discharge flow*

As illustrated in Fig. 13, the discharge flow of a three screw pump is calculated as the difference between the kinematic flow, the compression flow and leakage. So causes of discharge flow pulsation can be divided into the following 3 parts (Goenechea, 2007).

1 Pulsation due to kinematic flow, which is caused by the theoretical discharge flow without leakage.
2 Pulsation due to compression flow, which is caused by the pressure difference between outlet and the last chamber, which begins to open in the high pressure outlet.
3 Pulsation due to leakage, which is caused by the gaps *L1*, *L2, L3* and *L4*.

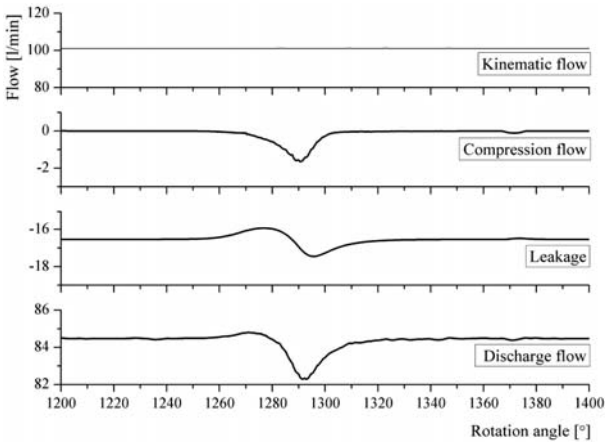

Fig. 14: *Causes of discharge flow pulsation*

Figure 14 illustrates the causes of the discharge flow pulsation of the test pump graphically. As was stated above, a three screw pump has no pulsation caused by kinemtic flow because a screw pump has the same cross section area and it is assured by the computed results. In addition, it can be assumed that a three screw pump has, compared to a piston pump, lower pulsation caused by compression flow and more pulsation caused by leakage. Due to the rise of pressure in the displacement chamber during transfer from inlet to outlet, the pressure difference is quite low at the point when the chamber is being connected to the outlet. This leads to a small backward flow into the chamber and relatively low pulsation caused by compression flow. But since the pump has a leakage change by pressure rise of the chamber opening in the outlet and by total resistance changes of gaps according to the rotation angle as shown by Fig. 5, there is the relatively high pulsation caused by leakage.

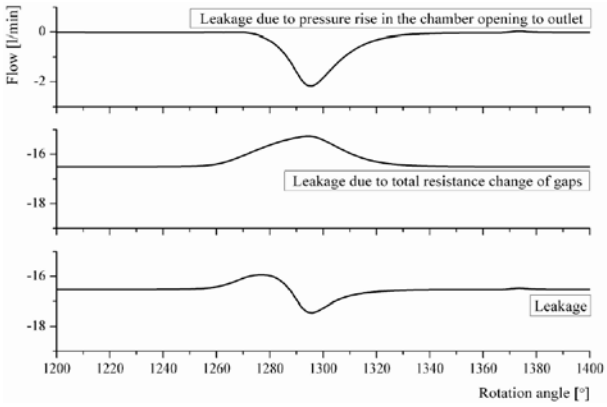

Fig. 15: *Causes of pulsation by leakage*

Figure 15 shows the different types of leakage that appear in a three screw pump. The leakage changes when the pressure in the displacement chamber which is opening to the outlet rises. Furthermore the leakage depends on the over-all resistance of the gaps which changes with the number of gaps between outlet and inlet. It can be seen, that the leakage change due to changing numbers of sealing gaps has a positive effect on pulsation. This leakage is contrary to the effects of compression flow (Fig. 14) and leakage due to pressure rise (Fig. 15). It can be explained by this reason that when a drive spindle in a three screw pump does not have the multiple length of the pitch (the total resistance of gaps depends on the length of a drive spindle), the pump has a lower pulsation as shown by Fig. 17.

5 Effects of Manufacturing Deviations

5.1 Length of Drive Spindle

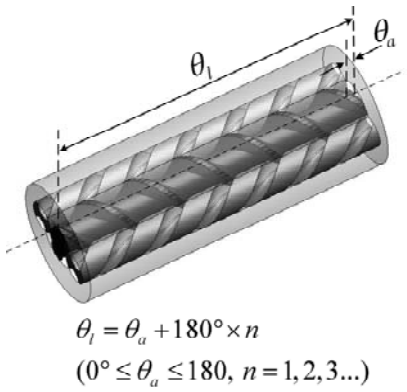

Fig. 16: *Length of drive spindle*

As previously stated, the total resistance change of gaps is one of the important parameters influencing the pressure pulsation of a three screw pump. This effect will be described in this paper. As illustrated in Fig. 16, the length of a drive spindle θ_l is defined by the sum of the angle of additional length θ_a and 180°× n.

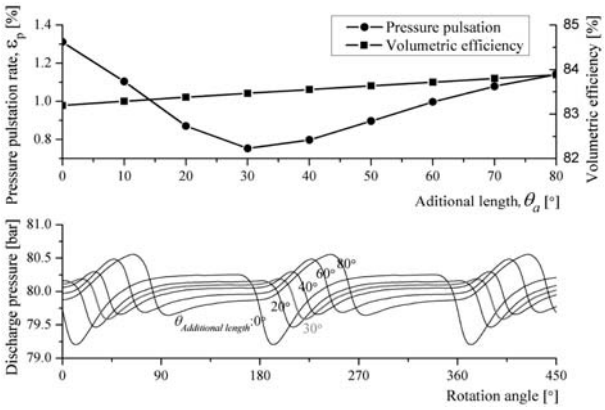

Fig. 17: *Pressure pulsation according to length of drive spindle*

Figure 17 shows the computed results of the pressure pulsation rate and the volumetric efficiency according to the rotation angle. To compare the computed results, the pressure pulsation rate was defined as follows.

$$\varepsilon_p = \frac{p_{max} - p_{min}}{p_{mean}} \tag{8}$$

Where p_{max} is the maximal discharge pressure, p_{min} is the minimal discharge pressure and p_{mean} is the mean discharge pressure.

The computed results show that the pressure pulsation can be reduced by using the optimized length of the drive spindle. Also the volumetric efficiency is improved. In case of this test pump, the 30° additional length of the drive spindle decreases pressure pulsation by about 0.56 % (0.45 bar in the discharge pressure of 80 bar). The volumetric efficiency increases by about 0.27 %. Deviation in dimension of 1 mm length of the drive spindle can cause an increase of the pressure pulsation rate of about 0.1 %. The results show that with increasing length of the drive spindle the positive effect on the leakage due to total resistance change of gaps which is described in Fig. 15 increases, too. The test pump used in this study has the additional length of about 30 °.

5.2 Diameter of Spindles and Sleeve

Deviations in diameters of spindles and sleeves directly influence the leakages *L1, L2, L3* and *L4*, so this deviation was considered in this study.

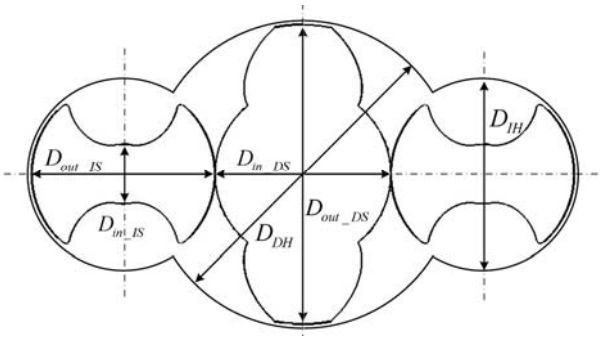

Fig. 18: *Configuration of spindles and sleeve*

Figure 18 shows the diameters of Spindles and sleeve, where D_{out_IS} denotes the outside diameter of idle spindle, D_{in_IS} is the inside diameter of idle spindle, D_{out_DS} is the outside diameter of a drive spindle, D_{in_DS} is the inside diameter of a drive spindle, D_{IH} is the diameter of the sleeve of the idle spindles and D_{DH} denotes the diameter of the sleeve of the drive spindle.

The diameters of spindles in a three screw pump follow theoretical relations according to Eq. (9).

$$\frac{D_{out\_DS}}{D_{out\_IS}} = \frac{5}{3},\ \frac{D_{in\_DS}}{D_{out\_IS}} = 1,\ \frac{D_{in\_IS}}{D_{out\_IS}} = \frac{1}{3} \tag{9}$$

Table 2 demonstrates that the diameters of the spindles in this test pump follow these relations with negligible differences.

Table 2: Diameter of spindles in the test pump

D_{out_DS}	38 mm
D_{in_DS}	22.4 mm
D_{out_IS}	23.3 mm
D_{in_IS}	7.65 mm

Table 3: Leakage changes according to diameter deviation of spindles and sleeve

Diameter \ Leakage		*L1*	*L2*	*L3*	*L4*
D_{out_DS}	- deviation	↑	-	-	↑
	+ deviation	↓	-	-	↓
D_{in_DS}	- deviation	-	↑	-	↓
	+ deviation	-	↓	-	↑
D_{out_IS}	- deviation	-	↑	-	↓
	+ deviation	-	↓	-	↑
D_{in_IS}	- deviation	-	-	-	↑
	+ deviation	-	-	-	↓
D_{DH}	- deviation	↑	-	-	-
	+ deviation	↓	-	-	-
D_{IH}	- deviation	-	↑	-	-
	+ deviation	-	↓	-	-

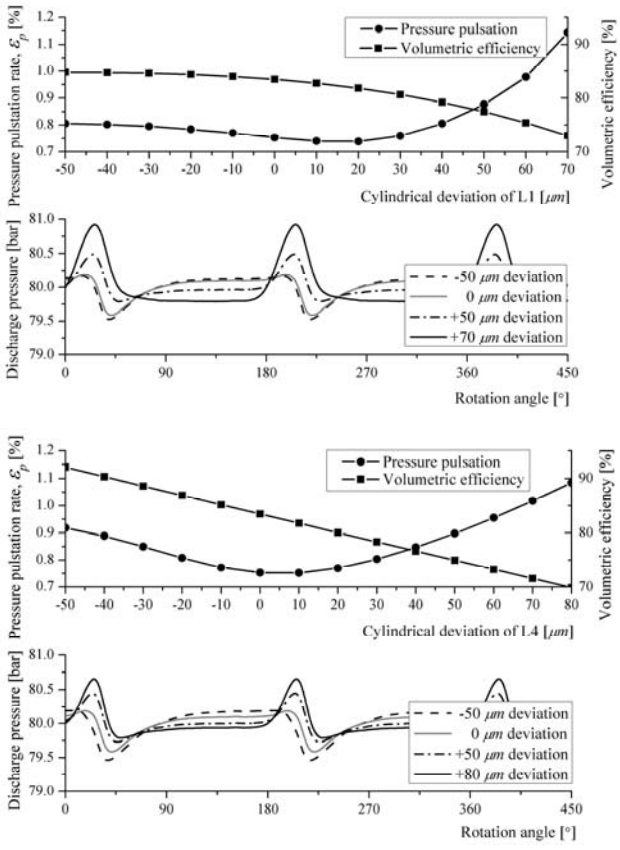

Fig. 19: *Pressure pulsation according to cylindrical deviation of L1 and L4*

Table 3 shows the changes of *L1, L2, L3* and *L4* according to the deviation in diameter of spindles and sleeve. For example, when the outside diameter of drive spindle D_{out_DS} increases, *L1* and *L4* decrease and when the inside diameter deviation of idle spindle D_{out_DS} increases, *L4* decreases.

The equation $D_{in\_DS} + D_{out\_IS} \geq D_{out\_DS} + D_{in\_IS}$ must always be satisfied. Then, D_{in_DS} and D_{out_IS} are in contact with each other caused by the resulting force of the pressure distribution between idle spindles and sleeve (Geimer, 1995).

To reduce the simulation time, instead of the simulation of pressure pulsation according to the diameter deviation of the spindles and sleeve, the pressure pulsation according to a cylindrical deviation of *L1* and *L4* is computed. Since the change of the pressure pulsation according to *L2* are similar to *L1* (the effect of *L1* on pressure pulsation is 3.6 times of *L2*), the effect of *L2* was not computed.

Computed results of the pressure pulsation according to the cylindrical deviation are plotted in Fig. 19. The calculated results show that an increase of *L1* and *L4* has an increasing effect on the leakage due to total resistance change of gaps similar to an increasing length of the drive spindle. In other words, if cylindrical deviation is increased, the overshoot of the outlet pressure caused by total resistance change of gaps increases and the undershoot decreases. So, for example, a deviation of 50 μm in cylindrical deviation of *L4* causes an increase of the pressure pulsation rate of about 0.15 % in the test pump.

5.3 Conical Spindles and Sleeve

The deviation in dimension of spindles and sleeve in a three screw pump can be conically shaped. Fig. 20 shows an example of a conical sleeve of the drive spindle. As shown by Fig. 19, since the difference of the pressure pulsations is slight when gaps are smaller (-cylinderical deviation) than the designed gaps, the case where gaps are larger than the designed gaps was only considered in this chapter. Therefore, if the cylindrical deviation at the high pressure side is higher than the designed gap, the conical shape was defined as positive. Otherwise, if the deviation at the low pressure side is higher, the conical shape was defined as negative.

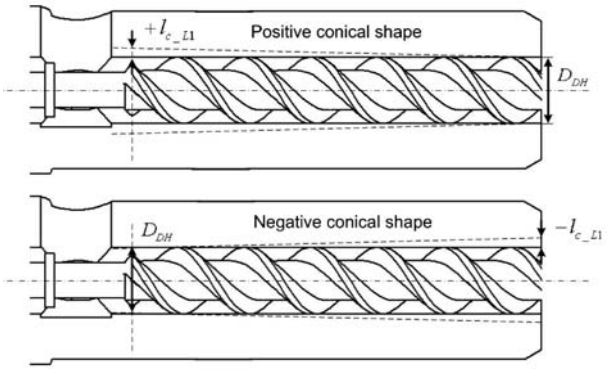

Fig. 20: *Conical sleeve of the drive spindle*

Figure 21 shows the computed results of the pressure pulsation depending on the conical deviation of *L1* and *L4*. The results show that if a pump has conical spindles or sleeves, the pump has different characteristics of pressure pulsation compared to a pump with the ideally cylindrical parts. If a pump has a positive conical shape, not only the positive effect of leakage due to total resistance change of gaps increases. There is also an influence on the pressure

during the range between overshoot and undershoot, when there is no change of the number of gaps. For example, as can be seen in Fig. 21 a positive conical shape (e.g. + 100 µm deviation of *L1*) leads to a falling pressure at a range of rotation angle from 90° to 180°.

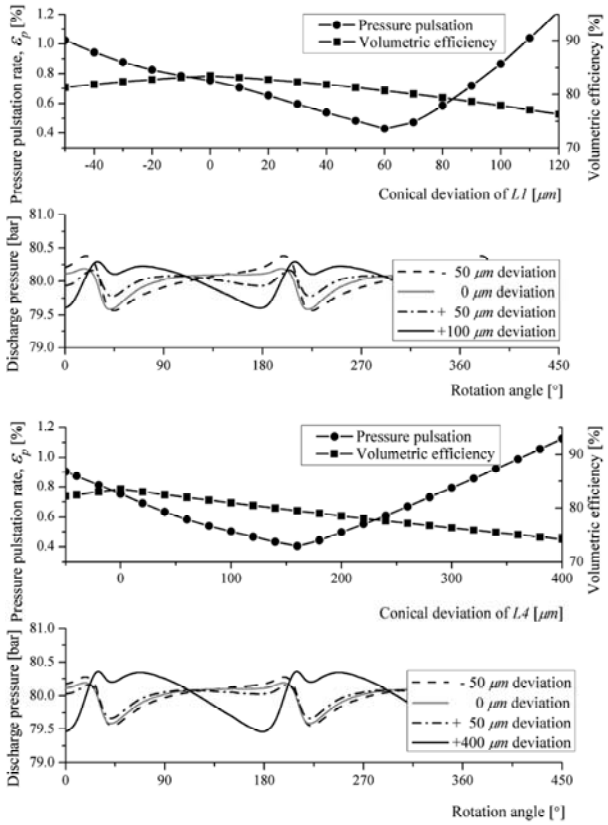

Fig. 21: *Pressure pulsation according to conical deviation of L1 and L4*

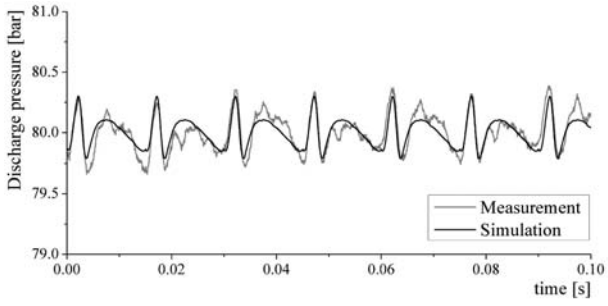

Fig. 22: *Comparison of the measured and calculated pressure pulsation of pump B*

The pressure pulsation can be reduced by using an optimal positive conical shape, but it is increased by a negative or large positive conical shape. In case of this test pump, 60 µm conical deviation of *L1* reduces the pressure pulsation rate by 0.32 %, but 100 µm conical deviation of *L1* increases the pressure pulsation rate by 0.11 %

Figure 22 demonstrates that the computed results with + 40 µm cylindrical and +50 µm conical deviation of *L1* can explain the pressure pulsation of the pump B very well.

5.4 Eccentricity of Idle Spindles

As a last step, the effect of eccentric spindles was considered. In most cases, the idle spindles have an eccentricity, as illustrated in Fig. 23. The eccentricity of an idle spindle can be defined by the eccentricity distance l_e between the center of its outside diameter and the center of its inside diameter. The eccentricity angle θ_e can be defined between the centreline of its outside diameter and the direction of the eccentricity.

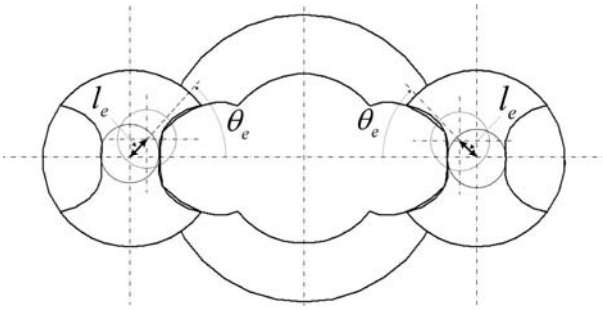

Fig. 23: *Configuration of eccentric idle spindles*

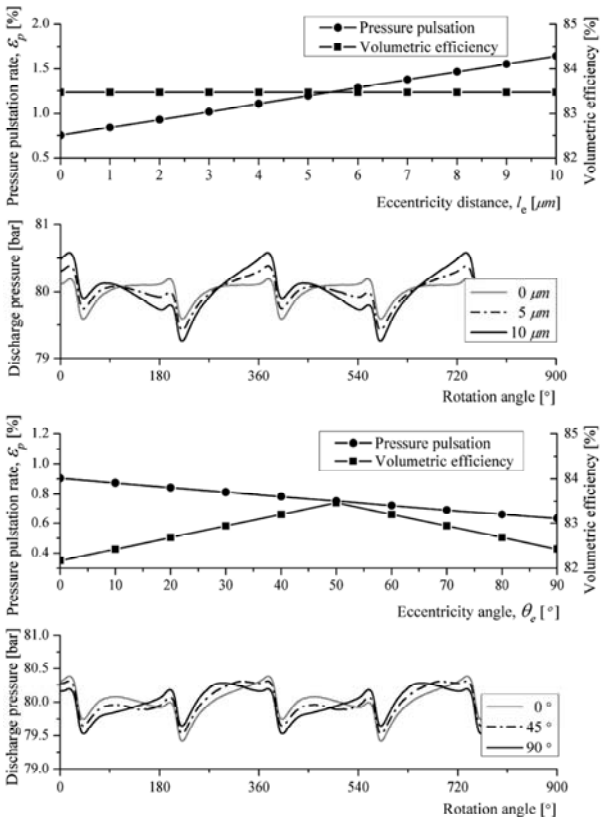

Fig. 24: *Pressure pulsation according to deviation of idle spindles*

Figure 24 shows the pressure pulsation depending on eccentricity distance and eccentricity angle. As shown by Fig. 24, the pressure pulsation is unsymmetrical due to an eccentric idle spindle and very sensitive to eccentricity. In case of this test pump, 10 µm eccentricity distance with 0° eccentricity angle increases the pressure pulsation by about 0.9 %.

The pressure pulsation of the pump C can be explained by an eccentricity of the idle spindles as demonstrated by Fig. 25. The parameters given in the simu-

lation model are as follows:

- - 40 µm cylindrical *L1* deviation;
- +20 µm conical *L1* deviation;
- One idle spindle with 15 µm eccentricity distance and 50° eccentricity angle;
- The other idle spindle with 15 µm eccentricity distance and 110° eccentricity angle.

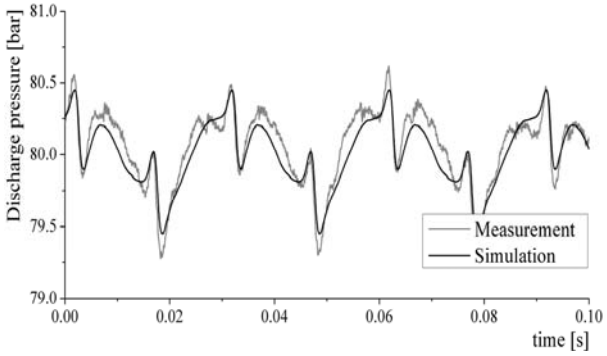

Fig. 25: *Comparison of the measured and calculated pressure pulsation of pump C*

7 Conclusions

This paper proved the problematic that the same pumps can have a different pressure pulsation due to deviation in dimensions. The reasons are cylindrical, conical and eccentric deviations of the spindles and the sleeve in between the range of manufacturing deviations. Precisely, when the length of the drive spindle or the cylindrical deviation between spindles and sleeve is increased, the overshoot of the pressure increases and the undershoot decreases. This is due to the fact, that leakage is dependent on the number of sealing gaps in the pump, which is not constant, as explained in chapter 4. The rising or falling pressure in the range between overshoot and undershoot can be explained by a conical gap between spindle and sleeve. The reason for an unsymmetrical pressure pulsation was identified to be eccentric deviations of the idle spindles. Especially it was found, that the eccentric deviation must be considered very carefully, because a three screw pump is very sensitive to eccentricity. The pressure pulsation can be reduced by choosing the optimal length of the drive spindle and a conical gap.

Table 3: Gap height and eccentric distance at 1 % pressure pulsation rate (about 33 % increase of the pressure pulsation rate compared to the original pump)

Cylindrical gap height	*L1*	125 µm
	L2	275 µm
	L4	140 µm
Conical gap height	*L1*	175 µm
	L2	465 µm
	L4	450 µm
Eccentric distance	*L4*	3 µm

In case of this test pump the gap heights which lead to a pressure pulsation rate of 1 % are given in Table 3. Therefore, with choosing the right manufacturing deviations the noise emission and efficiency of a three screw pump can be improved. The simulation model can be used to optimize the pressure pulsation.

Nomenclature

C_{sd}	chamber formed by drive spindle and sleeve	[-]
C_{is}	chamber formed by idle spindle and sleeve	[-]
D_{in_DS}	Inside diameter of drive spindle	[mm]
D_{in_IS}	Inside diameter of idle spindle	[mm]
D_{DH}	Diameter of sleeve for drive spindle	[mm]
D_{IH}	Diameter of sleeve for idle spindle	[mm]
D_{out_DS}	Outside diameter of drive spindle	[mm]
D_{out_IS}	Outside diameter of idle spindle	[mm]
E_{Fl}	Effective bulk modulus	[bar]
h_i	Gap heigh of chamber i	[um]
l_i	Gap width of chamber i	[mm]
l_c	Conical deviation	[µm]
l_e	Eccentricity distance	[µm]
L1	Leakage between sleeve and outside of drive spindle	[l/min]
L2	Leakage between sleeve and outside of idle spindles	[l/min]
L3	Leakage between inside of drive spindle and outside of idle spindles	[l/min]
L4	Leakage between outside of drive spindle and inside of idle spindles	[l/min]
p_{ci}	Pressure of chamber i	[bar]
p_d	Discharge pressure of the pump	[bar]
p_{R1}	Pressure of first RALA sensor	[bar]
p_{R2}	Pressure of second RALA sensor	[bar]
p_s	Suction pressure of the pump	[bar]
p_2	Pressure between RALA and pressure relief valve	[bar]
Q_C	Flow between a chamber and port	[l/min]
Q_L	Leakage of a chamber	[l/min]
α	Angle of begin to form a chamber	[°]
α_D	Orifice coefficient	[-]
η	Dynamic viscosity	[Pa s]
ε_e	Pressure pulsation rate	[%]
θ_a	Angle of additional length of drive spindle	[°]
θ_e	Eccentricity angle	[°]
θl	Angle of drive spindle length	[°]
ρ	Density of Oil	[kg/m^3]

References

Feist, M. 1976. Drücke rauf-Geräusche runter. Fortschritte bei Schraubenspindelpumpen. *Fluid. 12.* pp. 24 - 27.

Geimer, M. 1995. Meßtechnische Untersuchung und Erstellung von Berechnungsgrundlagen zur Ermittlung der Einsatzgrenze dreispindeliger Schraubenpumpen. RWTH Aachen

Goenechea, E. 2007. Mechatronische Systeme zur Pulsationsminderung hydrostatischer Verdrängereinheiten. RWTH Aachen

Ryanzantsev, V. M. 2000. Operation of a three screw pump on diesel fuel. *Chemical and Petroleum Engineering*. Vol. 36, Nos. 1-2, pp. 94 - 98.

Wegener, J. 1985. Screw pumps of one, two and three screw design. *2nd International Pump Symposium*. Texas, USA, pp. 41 - 46.

Willibald, K. 1992. Geräuschminderung an rotierenden Verdrängerpumpen insbesondere Schraubenspindelpumpen. *AFK.* pp. 135 - 147.

Sunghun Kim
Born on May 11th, 1977 in Korea. He received his degree in Mechanical Engineering with focus on Engineering Design from Korea Aviation University in 2004. After his graduation, he worked at the Korea Institue of Machinery and Materials (KIMM). And since 2007, he is member of the scientific staff of the Institute for Fluid Power Drives and Controls (IFAS) at RWTH Aachen University. His present research interests include hydraulic pump technology.

Ulf Piepenstock
Born on August 15th, 1978, he received his degree in mechanical engineering (Dipl.-Ing.) at RWTH Aachen University, Germany in 2005. Since 2005 he has been a member of the scientific staff and since 2006 he has been head of the research group “Pump and Motor Technology” at the Institute for Fluid Power Drives and Controls (IFAS) at RWTH Aachen University.

Hubertus Murrenhoff
Born on August 13th, 1953 in Germany, he is director of the Institute for Fluid Power Drives and Controls (IFAS) and dean of faculty of mechanical engineering at RWTH Aachen University, Germany. Main research interests cover hydraulics and pneumatics including components and the applications of fluid power in mobile and stationary equipment.